# Strain-resolved de-novo metagenomic assembly of viral genomes and microbial 16S rRNAs

Annika Jochheim[1,2], Florian A. Jochheim[2,3], Alexandra Kolodyazhnaya[1], Étienne Morice[1,2], Martin Steinegger[4,5,6,*], and Johannes Söding[1,2,7,*]

[1]Quantitative and Computational Biology, Max-Planck Institute for Multidisciplinary Sciences, Göttingen, Germany
[2]International Max-Planck Research School for Genome Sciences, University of Göttingen, Germany.
[3]Dep. of Molecular Biology, Max-Planck Institute for Multidisciplinary Sciences, Göttingen, Germany
[4]School of Biological Sciences, Seoul National University, Seoul, South Korea
[5]Artificial Intelligence Institute, Seoul National University, Seoul, South Korea
[6]Institute of Molecular Biology and Genetics, Seoul National University, Seoul, South Korea
[7]Campus Institute Data Science (CIDAS), University of Göttingen, Germany.
[*]Correspondence: martin.steinegger@snu.ac.kr, soeding@mpinat.mpg.de

March 29, 2024

**Abstract**

Metagenomics is a powerful approach to study environmental and human-associated microbial communities and, in particular, the role of viruses in shaping them. Viral genomes are challenging to assemble from metagenomic samples due to their genomic diversity caused by high mutation rates. In the standard de Bruijn graph assemblers, this genomic diversity leads to complex $k$-mer assembly graphs with a plethora of loops and bulges that are challenging to resolve into strains or haplotypes because variants more than the $k$-mer size apart cannot be phased. In contrast, overlap assemblers can phase variants as long as they are covered by a single read. Here, we present PenguiN, a software for strain resolved assembly of viral DNA and RNA genomes and bacterial 16S rRNA from shotgun metagenomics. Its exhaustive detection of all read overlaps in linear time combined with a Bayesian model to select strain-resolved extensions allow it to assemble severalfold more viral strain genomes and 16S rRNAs from various real and simulated short-read datasets than the state of the art.

## 1 Introduction

In shotgun metagenomics, DNA from environmental samples is directly sequenced, usually with short-read sequencing techniques. Millions to billions of short reads per sample are assembled into contigs, which are then binned into hundreds of different metagenome-assembled genomes. This approach circumvents the need to cultivate microbes in the lab, which requires to painstakingly search for suitable cultivation conditions for each microbial species. The ease of accessing the composition and gene-encoded functions of microbes with these cultivation-independent techniques have therefore greatly propelled progress in environmental microbiology [1] and particularly in medical research, where ever tighter links are being discovered between our gut-associated microbiomes and the development and homeostasis of our immune system, our metabolic health, and the normal functioning of our brains [2, 3, 4].

Viruses infecting bacteria or archaea (called phages) have recently moved into the limelight, as their central roles in shaping environmental and gut microbiomes are becoming clearer. Phages are particularly difficult to study in the lab because their prokaryotic hosts are often difficult to cultivate themselves and, on top, propagating viruses in the lab requires finding conditions that may well be distinct from those used to cultivate their hosts [5]. Therefore, viral metagenomics has greatly accelerated the study of phages and their roles in shaping environmental and animal- and plant-associated microbial ecosystems, such as soil [6, 7, 8], aquatic environments [9, 10, 11,

12, 13, 14], or the human gut [15, 16, 17, 18]. These and other studies indicate that phages have a huge impact on their host communities, by shaping their compositions and dynamics and driving bacterial diversity [19, 20]. However, only a minute sliver of the world's virome has so far been discovered [21].

Virus genomes can be retrieved from datasets enriched for virus particles (viral metagenomes) or from bulk metagenomes, including both virus particles and microbial cells [22, 5]. Resolving viral genomes from metagenomic data is challenging. Viruses have small sizes and therefore often represent only a minor fraction of the reads, whereas the background contamination from bacterial or eukaryotic hosts can be high [23, 24]. The chief difficulty stems from the high microdiversity and strain heterogeneity resulting from an error prone replication process, the lack of repair mechanisms, and the frequent exchange of genomic segments [25, 26].

Genomic assembly follows one of two approaches [27]: In overlap assembly, one computes the overlap alignments between all reads, links reads with sufficient overlap and similarity in their overlapping regions, and constructs contiguous assembled sequences (contigs) from chains of linked reads. This approach dominated until short read sequencers producing millions of reads became popular and the quadratic runtime for computing all-versus-all alignments became prohibitive. In de Bruijn graph assembly, one constructs a graph in which each node represents a $k$-nucleotide subsequence ($k$-mer) and edges are drawn between successive $k$-mers in a read. Contigs are constructed from paths through this de Bruijn graph. Because no all-versus-all alignment of reads is required, the runtime scales only linearly in the nunmber of input reads. For this reason, modern metagenomics assemblers (except Plass [28]) employ de Bruijn graphs [29, 30, 31].

However, this efficiency gain comes with the downside that genomes of closely related strains cannot be resolved. Beyond the distance of the maximum $k$-mer size, which is typically around 55, the information whether two variants occurred in the same read is lost when reducing the reads to a de Bruijn graph (Fig. **1**B). Genomes with average nucleotide identity (ANI) $\geq 95\%$ have many identical stretches longer than the typical $k$-mer size. The $k$-mer size is limited by the quickly exploding complexity of the de Bruijn graph for increasing $k$ due to intra-strain microdiversity in microbial populations and sequencing errors. Therefore, most de Bruijn graph assemblers only attempt to assemble consensus genomes instead of strain-resolved genomes.

Viral populations with their high microdiversity and strain heterogeneity pose formidable challenges to assembly of viral genomes from metagenomic data. The resulting complex graph structures lead to fragmented assemblies and make the reconstruction of strain-resolved genomes even harder [32]. State-of-the-art metagenomic viral assemblers metaviralSPAdes [33], rnaviralSPAdes [34], and Phables [35] employ various heuristics to simplify the graph structure, for example by removing tips, bubbles, and bulges with low coverage. To resolve strains, Phables, rnaviralSPAdes, and Haploflow [36] employ flow decomposition: They find a set of paths and read coverages that would add up to approximately the read coverages observed in the de Bruijn graph. Unfortunately, flow decomposition has less utility for virus genomes due to their uneven read coverage, particularly for RNA phages, for which the reverse transcription step introduces strong sequence biases [37].

Several tools have been developed for the assembly of viral genomes in patient samples, which typically contain a small number of highly similar strains. Haplotype assemblers Haploflow, SAVAGE [38], and MLEhaplo[39] aim to reconstruct strain-resolved genomes, while IVA [40] and VICUNA [41] reconstruct consensus genomes. All except Haploflow are overlap assemblers, which make use of the co-occurrence of mutations within reads. However, they were not designed to analyse complex metagenomic dataset and also tend to be much slower than de Bruijn graph assemblers.

Assembly of 16S rRNA genes from metagenomic data is of particular interest because of their use as marker genes in the identification, quantification, and phylogenetic analysis of prokaryotes. Assembling 16S rRNA genes is a problem analogous to strain-resolved viral genome assembly. Like genomes of related viral strains, 16S rRNA genes of have highly conserved regions interspersed with regions of higher variation. The highly conserved regions are longer that the typical $k$-mer length and hence de Bruijn graph assemblers cannot know how to connect these variable regions across the conserved ones. This results in highly branched de Bruijn graphs, making the reconstruction of individual 16S rRNA gene sequences hard [42, 43]. Usually, either 16S sequences of several species are merged into consensus sequences or assemblies remain very fragmented [44].

Here, we present PenguiN, a de-novo metagenomic overlap assembler for viral genomes and 16S rRNA genes. PenguiN iteratively extends reads and growing contigs by computing all overlap alignments between them and selecting the extensions that are most likely to be from the same

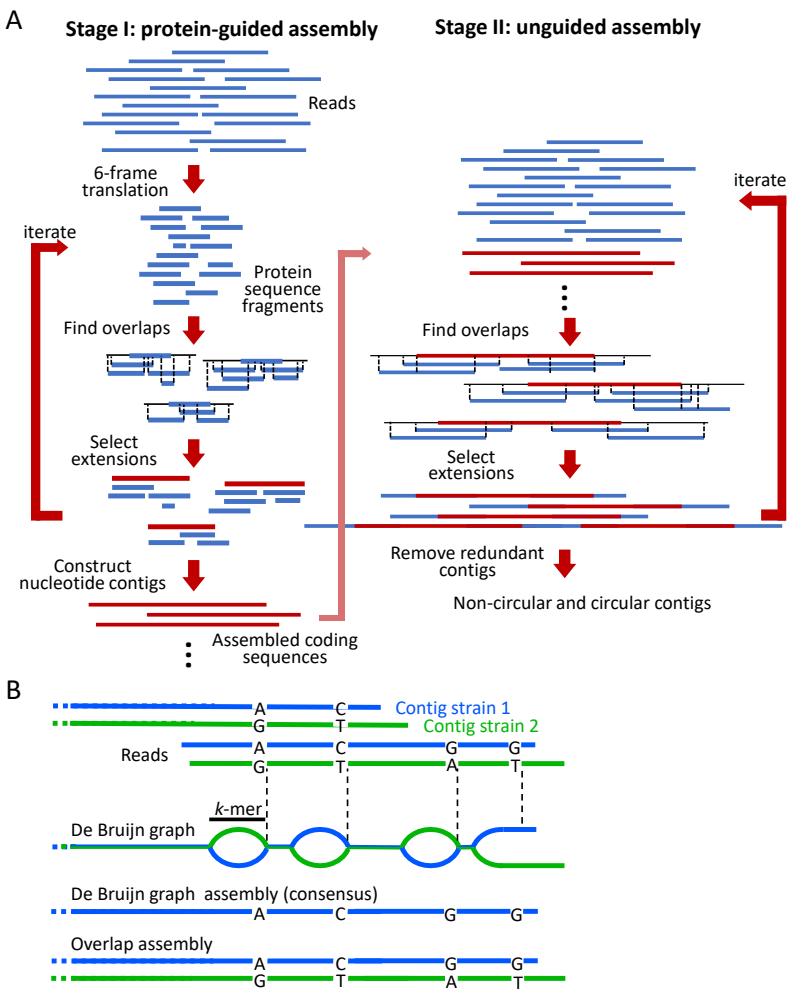


**Figure 1**: **PenguiN overview.** (**A**) PenguiN assembly proceeds in two stages: (I) protein-guided assembly of coding regions, and (II) nucleotide assembly to link coding regions. In each stage, sequences are iteratively extended by computing overlap alignments in linear time, ranking possible extensions by their quality, and extending upstream and downstream with the best sequence. (**B**) De Bruijn graph assemblers cannot resolve strains across conserved regions longer than their $k$-mer length (black bar). In contrast, overlap assemblers like PenguiN can link strain assemblies correctly across all conserved regions shorter than the read length.

strain, based on a novel Bayesian statistical model. Similar to Plass [28], our protein-level assembler, PenguiN achieves fast speeds and a linear run time complexity by applying Linclust [45], the first algorithm to cluster protein and nucleotide sequences in linear time. To gain robustness with respect to the high level of microdiversity in viral genomes, PenguiN guides its nucleotide assembly by evaluating the protein sequences when merging coding sequences. On simulated and real complex metagenomic short read datasets, PenguiN assembled several times more viral genomes and 16S RNAs at similar error rates than nine state-of-the-art metagenomic or viral assemblers.

# 2 Results

## Overview of PenguiN

PenguiN is an overlap assembler that uses two largely analogous stages. In stage I (Fig. 1A left), it assembles six-frame translated reads into proteins, while also co-assembling the corresponding nucleotide coding sequences. In stage II (Fig. 1A right), it links the contigs covering coding regions obtained from stage I across non-coding regions. PenguiN follows a greedy iterative assembly scheme. Like our protein-level assembler Plass [28], it uses the Linclust algorithm [45] to find signif-

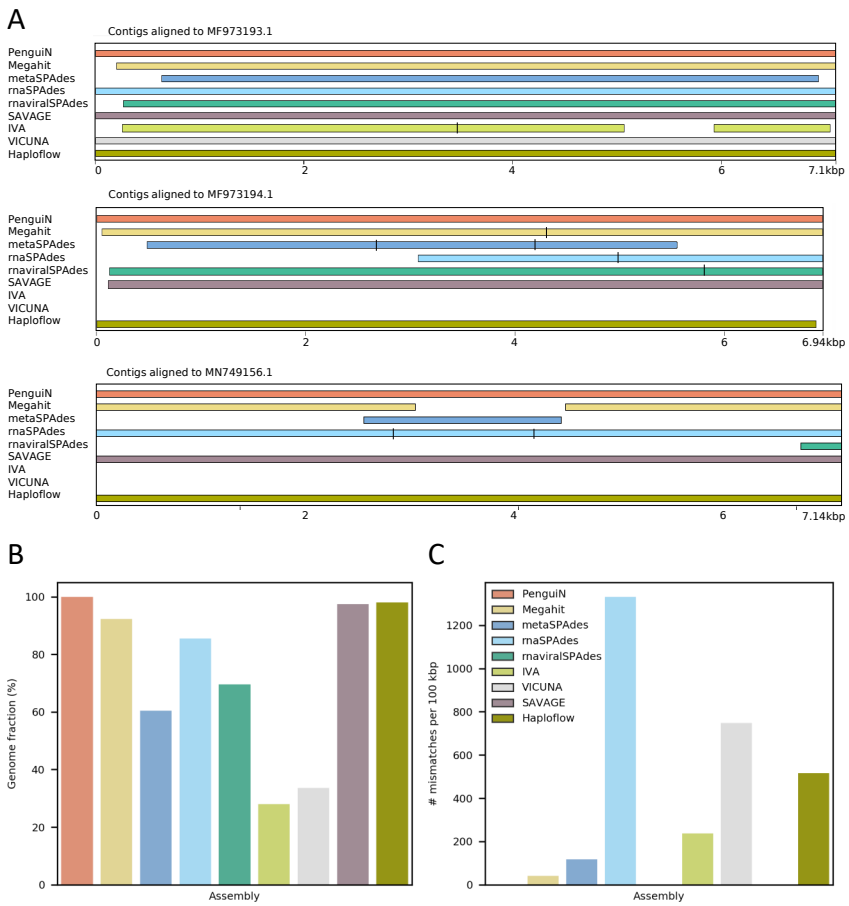


**Figure 2**: **Assembly quality on an in-silico mixture of three HRV genomes.** (**A**) Comparison of three genomes assembled by the nine assemblers aligned to the reference. Black bars indicate fragmentation where contigs overlap. (**B**) Fraction of the three genomes covered and (**C**) number of mismatches, computed by MetaQUAST [46].

icant overlaps in linear time and extends the sequences iteratively. To avoid chimeric extensions, for each center sequence, we select from several possible extensions the one with the highest Bayesian posterior probability to belong to the same genome (see Methods). When overlap lengths differ, this scheme improves upon the Plass extension strategy of choosing the overlap with the highest sequence identity. Both stages perform multiple iterations of overlap computation and extension. In addition, in stage II we detect circular sequences after each extension (see Methods), because plasmids and many viral genomes are circular. We exclude them from further iterations to avoid over-extension and mark them for the final results. Finally, the resulting contigs are clustered and one representative per cluster is selected to reduce redundancy.

Using full-read overlaps to find the best extensions enables PenguiN to perform strain-level assemblies, a task that standard $k$-mer-based de Bruijn graph assemblers struggle with (Fig. 1B). Many perfectly conserved regions between two strains will be longer than their $k$-mer length, since strains typically have sequence identities between 90% and 99%. De Bruijn graph assemblers have no way of telling which contig upstream of such a conserved region should be joined to which contig downstream. Therefore, these assemblers either fragment the assembly at the conserved regions to avoid generating chimeric contigs, or they resort to assembling the consensus genome. In contrast, PenguiN can use the full overlap alignment and information about co-occurring mutations to select the best extension and assemble the genomes of strains (Fig. 1B).

We tested PenguiN on synthetic and real datasets and compared it to state-of-the-art assembly tools, both de Bruijn graph and overlap-based.

## Assembly of an in-silico mixture of HRV genomes

We first generated a synthetic dataset comprised of three human rhinovirus strains (see Methods). We simulated $2 \times 150$ bp error-free reads from the three genomes using randomreads.sh from the BBMAP software suite in proportions 4:2:1 with coverages of 200, 100 and 50, respectively. The genomes have average nucleotide identities (ANI) ranging from 92% to 95%, with mismatches mainly due to single-nucleotide polymorphisms (SNPs). We assembled them using PenguiN and nine other assemblers: Megahit [29], metaSPAdes [30], metaviralSPAdes [33], rnaSPAdes [31], rnaviralSPAdes [34], SAVAGE [38], IVA [40], VICUNA [41] and Haploflow [36]. MetaviralSPAdes did not produce any assemblies and was excluded from the subsequent analysis. Assembly quality was assessed using MetaQUAST [46]. The results are shown in Fig. **2** and the MetaQUAST report is available in Additional File 1: Fig. S1.

PenguiN performed well in all metrics. It assembled three contigs, covering almost 100% of all three strain genomes with a single contig each (Fig. **2**A, B). Two further assemblers assembled all three strain genomes to a high degree of completeness: Haploflow (97.98%) and SAVAGE (97.39%). All other assemblers only assembled the most frequent strain completely, while either fragmenting or missing parts of the other two. For example, Megahit recovered only 80% of the strain with the lowest abundance (MN749156.1), metaSPAdes recovered merely 20%, and rnaviralSPAdes only 15%. IVA and VICUNA, which were designed to assemble viral quasispecies, both assembled a consensus genome, that could only be aligned to the most abundant genome by MetaQUAST.

MetaQUAST reported no misassemblies for any of the tools, but half of them generated assemblies with a significant number of mismatches or indel errors (Fig. **2**C, Additional File 1: Fig. S1), indicating a mixture of the strains.

## Performance on highly diverse strain mixtures

Next, we aimed to construct a more challenging dataset with a very high degree of natural variation. To this end, we used 2550 HIV-1 genomes from the NCBI database (see Methods). The HIV-1 genome is approximately 9.7 kbp and has long terminal repeats (LTRs) at both ends, due to which the genome can be both in linear and circular form [47, 48]. We used the circularized forms of all genomes as the ground-truth reference (see Methods), since all linear assemblies can be perfectly mapped to them. The pairwise nucleotide identities among the 2550 genomes are mostly in the range of 85% to 95% (Fig. **3**A). We generated synthetic datasets with $2 \times 150$ bp error-free reads with overlap lengths uniformly distributed between 40 and 60 nucleotides. To analyse the dependence of the assembly quality on genomic coverage, we generated in total three datasets of reads with mean coverage of each genome set to 1×, 10×, and 100×. Due to the high number and similarity of the genomes, this dataset was particularly challenging to assemble.

SAVAGE de novo and Haploflow did not finish within 10 days at 10× and 100× coverage and could not be evaluated. MetaviralSPAdes, IVA, and VICUNA produced only very few or no contigs. We again evaluated the assembly quality using MetaQUAST [46]. PenguiN performed best in most metrics (Fig. **3**B-D). The distribution of the fractions of assembled genomes shows that PenguiN assembled several times higher genome fractions across all coverage values than the next best tool, rnaSPAdes (Fig. **3**B). The median assembled genome fractions for PenguiN at 10 and 100 times coverage were 86% and 97%, respectively, compared to 28% and 34% for rnaSPAdes (Fig. **3**C). On the low coverage set, PenguiN was the only tool able to recover genomes with a fraction of more than 90%. The analysis was performed using the MetaQUAST default threshold of 95% sequence identity. In total, PenguiN recovered 27 genomes by more than 90% on the 1× coverage set, 1136 on the 10× coverage set, and 1550 genomes on the 100× coverage set, whereas the next best tools rnaSPAdes and Megahit recovered 0, 24, and 36 and 0, 3 and 11 respectively, corresponding to an approximately 40-fold increase.

PenguiN's genome assemblies also consist of much longer contigs, as measured by NGA50. While almost all assemblers can gain from more coverage, most assemblers except for PenguiN either have fragmented assemblies or do not cover the reference genomes with $\geq 50\%$ (counted as NGA50=0). At 10 and 100 times coverage, 50% of the 2550 genomes assembled by PenguiN had NGA50 values above 3.6 kbp and 5.7 kbp, respectively, while the next best tool in this regard, rnaSPAdes, had only 22 and 12 genomes with NGA50 values above these lengths (Fig. **3**D).

Also, PenguiN's number of misassemblies per contig was the second best on the 1× and 10×

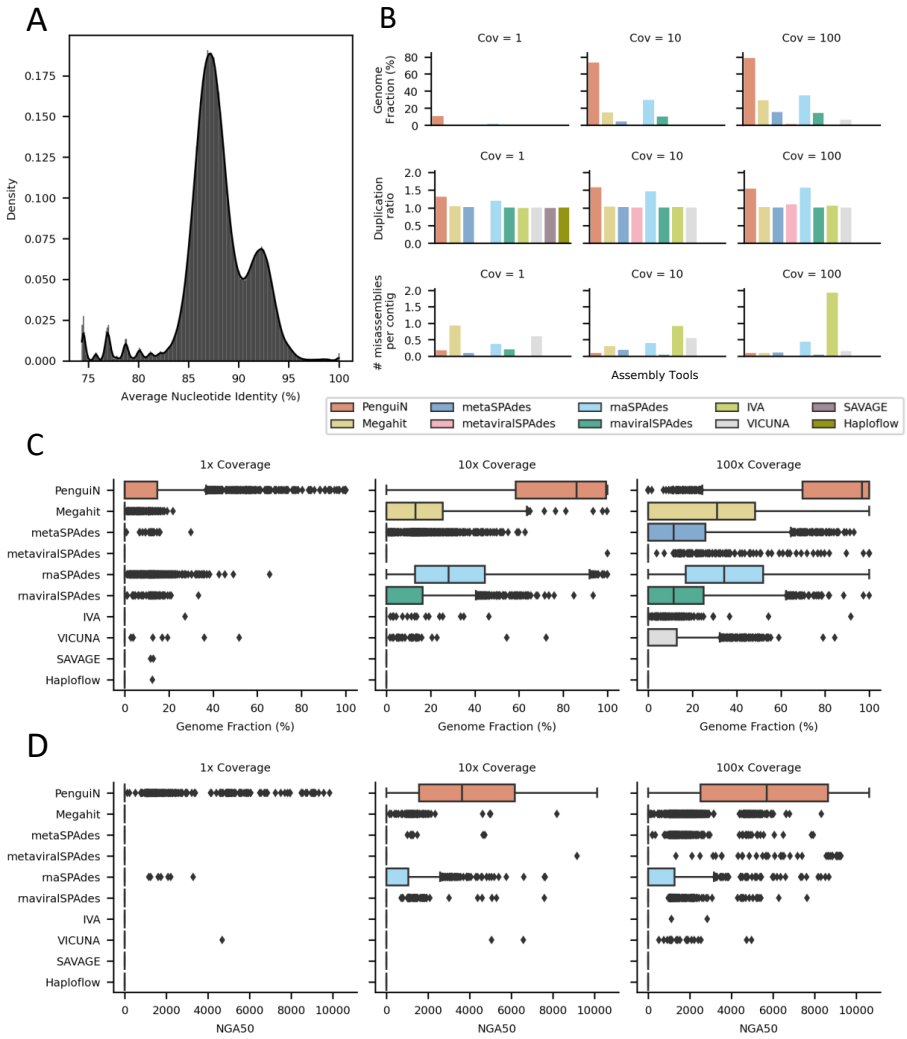


**Figure 3**: **Assembly quality on an in-silico mixture of 2550 HIV-1 genomes** on three datasets with an average coverage of each genome of 1×, 10×, and 100×. (**A**) Distribution of pairwise sequence identities among the 2550 HIV-1 genomes. (**B**) Average assembled genome fraction, number of misassemblies per contig, and duplication ratio. (**C**) Distribution of the fractions of each of the 2550 genomes covered by the assemblies. (**D**) Distribution of the NGA50 values. The NGA50 value of a genome assembly is the length for which contigs of that size and longer cover 50% of the genome. The larger the NGA50 value is, the less fragmented is the assembly.

coverage dataset, and the third best on 100× coverage dataset. Especially, it was significantly lower than rnaSPAdes, the assembler with the second best completeness. On the flip side, the high completeness of PenguiN assemblies resulted in a higher duplication ratio (between 1.3 and 1.6) than for other tools except rnaSPAdes (Fig. **3**B).

To gain a deeper insight into the assembled diversity, we assessed how the assembly quality depends on the stringency of the mapping of contigs to reference genomes. We mapped the contigs assembled by each tool with MMseqs2 [49] to the 2550 reference genomes. We recorded the per-base sensitivity of the assembled contigs, requiring a minimum sequence identity of $x$% for the alignment between the contig and the mapped reference sequence (Fig. **4**). At 90% sequence identity mapping stringency, all tools achieve close to 100% sensitivity on the coverage 100 dataset. This means that for any reference genome, all tools are able to assemble contigs that together cover the entire genome with at least 90% sequence similarity. The same contig can be mapped to multiple references. However, PenguiN's sensitivity decreases much more slowly with increasing stringency than the other tools, demonstrating that it was able to assemble much more of the strain variation in this dataset. At the highest sequence identity cutoff (X=99%), PenguiN correctly assembled approximately 3-6 times more nucleotides than the next best tool rnaSPAdes (1× coverage: 9.6%

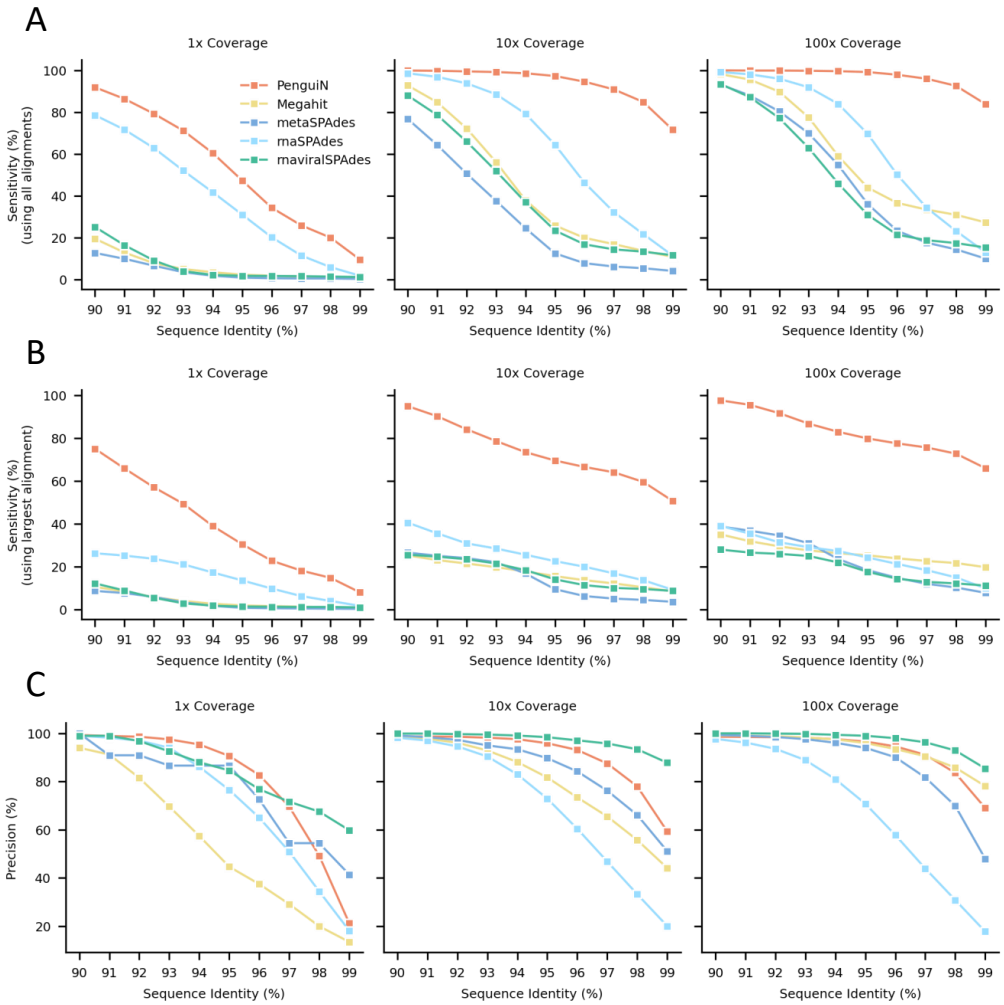


**Figure 4**: **Per-base sensitivity and precision of assemblies generated for the 2550 HIV1 genomes dataset**. (**A**) Fraction of nucleotides in the reference genomes that are aligned to an assembled contig with a sequence identity at least the value on the $x$-axis. (**B**) Fraction of nucleotides of the reference genomes that are aligned to the longest contigs in the assembly that has a sequence identity of at least the value on the $x$-axis. (**C**) Assembly precision is the fraction of assembled nucleotides contained in alignments to a reference genome with sequence identity at least the value on the $x$-axis.

vs. 1.9%; 10× coverage: 71.6% vs. 11.5%) or Megahit (100× coverage: 83.9% vs. 27.4%). This is in accord with the analysis by MetaQUAST in Fig. 3B.

When only considering the longest alignment per reference genome instead of all alignments, the difference in sensitivity between PenguiN and the other assemblers becomes even more pronounced across all sequence identity cutoffs (Fig. 4B). Consistent with the NGA50 analysis, this result reflects the much lower level of fragmentation within PenguiN's assemblies.

To analyse whether the much longer contigs assembled by PenguiN would lead to a higher fraction of chimeric contigs or misassemblies, we also calculated the per-base precision of the assembled contigs at different stringencies of sequence identity mapping (Fig. 4C). For all three coverage sets (1×, 10×, 100×) and over the entire range of sequence identities, PenguiN's precision is close to the second best tool or second best itself, except at coverage 1 and sequence identity $\geq 98\%$, where Megahit and rnaviralSPAdes are significantly more precise but assemble 34 and 50 times fewer nucleotides than PenguiN, respectively. Only rnaviralSPAdes has markedly better precision everywhere, but this comes at the cost of very low sensitivities. At $X = 99\%$ sequence identity, 21.2%, 59.3%, and 69% of PenguiN's contigs could still be aligned to a reference genome sequence in the 1×, 10×, and 100× coverage datasets, respectively. These results show that although PenguiN assembles much longer contigs than the other tools, it does not systematically produce

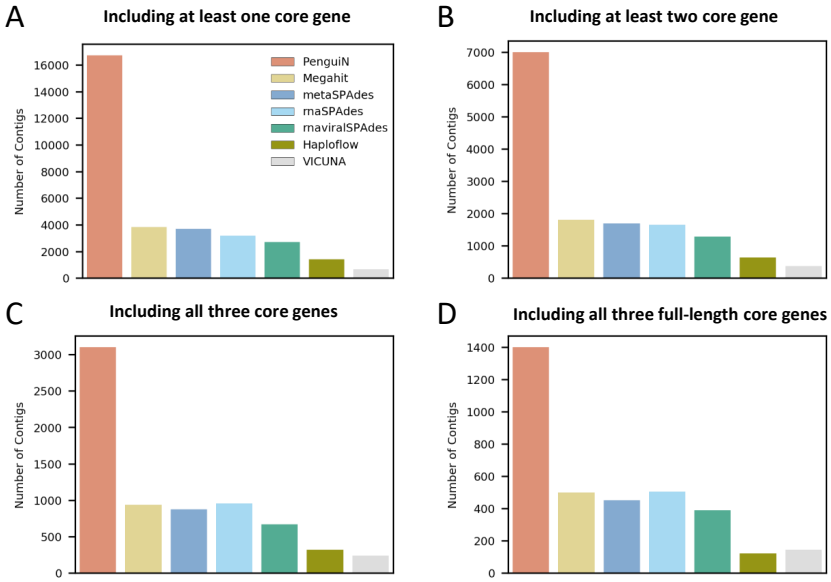


**Figure 5**: **Number of contigs of non-redundant ssRNA phage genomes assembled from 82 environmental metatranscriptomic samples.** Profile HMM searches identified contigs containing matches to at least one of the three core proteins of ssRNA phages (MP, CP, RdRp). Contigs were redundancy-filtered at 99% pairwise sequence identity. (**A**) Contigs containing a match to at least one of the three core proteins. (**B**) Contigs containing matches to at least two core proteins. (**C**) Contigs containing matches to all three core proteins. (**D**) Contigs containing full-length matches to all three core proteins ("complete genomes").

more missassemblies.

## Assembly of ssRNA phages from real metatranscriptomic samples from activated sludge and aquatic environments

Next, we tested the assemblers on 82 metatranscriptomics samples from activated sludge and aquatic environments, which were recently presented in a study to detect ssRNA phages from these two environments [50]. The challenge in comparing assemblers on real metagenomic data is the lack of a ground truth. Single-stranded RNA (ssRNA) bacteriophages offer a solution, as they occur only in two relatively narrow families, Leviviridae and Levi-like viruses [51]. All of them have a short, positive-stranded genome of 3.5 kbp-4.5 kbp that contains three core proteins, a maturation protein (MP), a coat protein (CP) and an RNA-dependent RNA polymerase (RdRp), as well as a few other facultative, short and much less conserved hypothetical proteins [52, 53, 50]. Since the three core proteins are always present, we could assess the completeness of assembled ssRNA phage genomes by whether they contain full-length versions of the three core proteins.

We assembled the 82 metatranscriptomic samples with PenguiN and the nine other tools and searched the contigs for matches to the profile Hidden Markov Model (HMM) that Callanan et al. [50] constructed by combining HMMs of the three core proteins. Assembly runs were performed on single nodes with two Intel Xeon E5-2640v3 2.6 GHz processors with a total of 16 cores and 128 GB of RAM. As before, the size and complexity of the data set posed problems for multiple assemblers. SAVAGE and IVA did not finish on any sample within 10 days. MetaviralSPAdes assembled only very few contigs with only one hit to the HMM profiles across samples. Haploflow and VICUNA did not finish within 10 days on 33 and 6 samples, respectively, and hence could not be evaluated on these. The runtimes of the assemblers, that finished on all samples, summed up to 3.7 days for PenguiN, 1.2 days for Megahit, 1.3 days for rnaviralSPAdes, 1.4 days for rnaSPAdes, and 27.8 days for metaSPAdes.

In total, we identified 29 106 non-redundant ssRNA phage sequences (see Methods) in the PenguiN assemblies across all samples, of which 4045 contain three complete core proteins ("complete genomes"). This number was four times higher than the 1015 complete ssRNA phage genomes

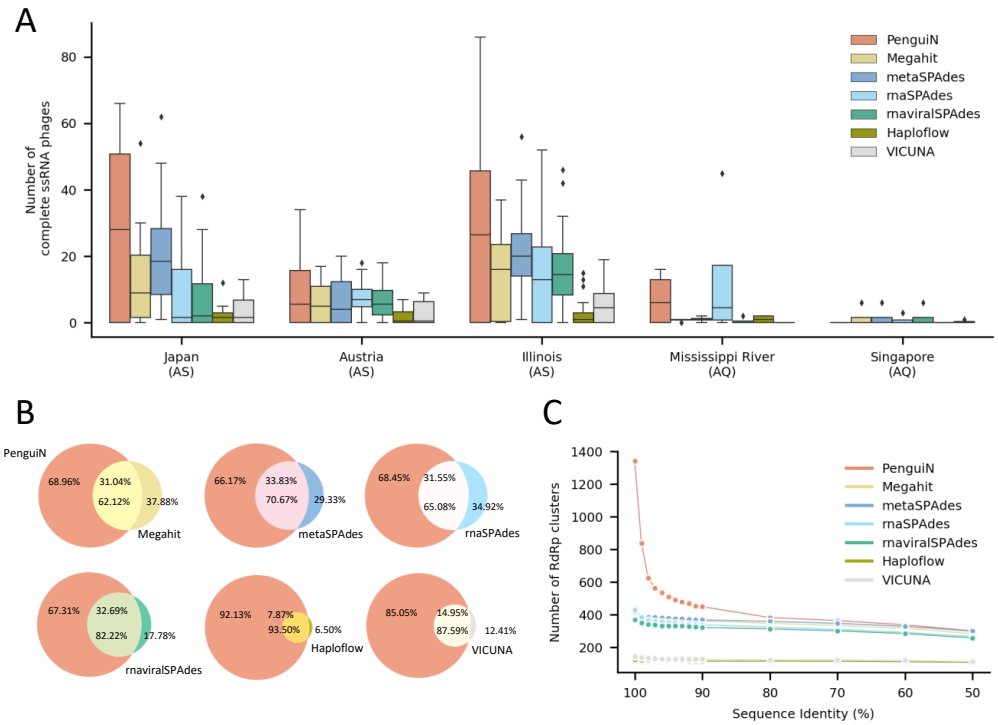


**Figure 6**: **Analysis of assemblies of ssRNA phage genomes from 82 metagenomic samples.** (**A**) Distributions of the numbers of complete ssRNA phage genomes for the three sampling locations for activated sludge (AS) and the two environmental freshwater samples that yielded ssRNA genomes (AQ). (**B**) Venn diagrams showing the fractions of contigs of PenguiN covered by contigs of one of the six other tools and contigs of these six tools covered by contigs of PenguiN. For a contig to be covered, at least 99% of its nucleotides must be contained in an alignment with at least 99% sequence identity. (**C**) Number of redundancy-filtered, complete RdRp proteins encoded in the assemblies as a function of stringency of redundancy filtering, the pairwise amino acid sequence identity cut-off.

reported in [50]. To avoid counting redundant versions differing by only a few mismatches due to sequencing errors or intra-population diversity, we clustered all contigs using MMseqs2 with a maximum sequence identity of 99% and counted only the non-redundant cluster representatives, when comparing PenguiN to the other assemblers. This resulted in 1398 "complete genomes" for PenguiN, three times more than for rnaSPAdes and Megahit. Figure **5**A-D compares the number of contigs assembled by PenguiN and the other assemblers at four levels of genome completeness: contigs with a match to a single, two or all three core proteins, and with full-length versions of the three core proteins. At all four completeness levels, PenguiN assembled at least twice as many contigs as the next best tools, Megahit and rnaSPAdes.

By far the most complete genomes per sample were assembled from activated sludge (samples from Japan, Austria, Illinois), as already reported by [50]. Here, PenguiN assembled 32% more complete genomes than the next best tool, while on the freshwater samples (Mississippi River, and freshwater aquatic samples from Singapore) it yielded a comparable number (Fig. **6**A). On the samples from Lake Mendota, none of the assemblers could reconstruct a complete phage sequence. We then analysed the intersections between each of the assembled sets of complete phage genomes (using redundancy-filtered at 99% identity and 99% coverage). The genomes of the three next best assemblers each covered only about one third of the genomes assembled by PenguiN, whereas Penguin covered about two thirds of their genomes (Fig. **6**B). This fraction was quite high considering that PenguiN is an overlap assembler and the other tools are de Bruijn graph assemblers which, among them, also attain fractions around 2/3 despite the similarity of their assembly approaches. The assemblies of Haploflow and VICUNA were even covered by PenguiN with 93.5% and 87.6%, respectively.

We asked whether the increased diversity observed in the genomes assembled by PenguiN was due to a higher number of genera, species, or strains. We extracted the RdRp genes from the

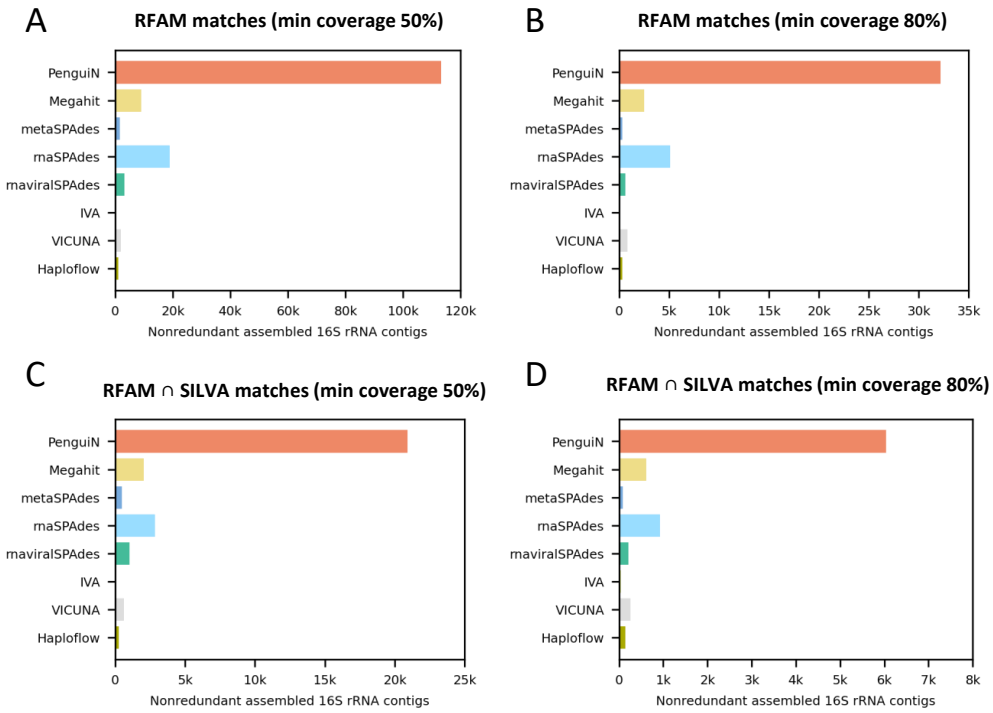


**Figure 7**: **Number of assembled 16S rRNA contigs matching RFAM entries.** (**A**) Nonredundant 16S rRNAs matching RFAM entries with at least 50% of coverage. (**B**) Nonredundant 16S rRNAs matching RFAM entries with at least 80% of coverage. (**C**) Nonredundant 16S rRNAs matching RFAM entries with at least 50% of coverage and having a match in SILVA database. (**D**) Nonredundant 16S rRNAs matching RFAM entries with at least 80% of coverage and having a match in SILVA database.

complete genomes and clustered the RdRp protein sequences at various levels of sequence identity. Using cutoffs for species (80% sequence identity) and genera (50%) found in [50], we saw a similar number of clusters for all assemblies (except VICUNA and Haploflow). However, at higher cutoffs, PenguiN's assembly showed many more clusters than the other tools, indicating increased strain-level diversity (Fig. **6**C). This was in accordance with our observation on the simulated datasets that Penguin resolved strains where other assemblers merged their genomes.

To check for chimeric assemblies, we considered the genome architecture within PenguiN's contigs classified as complete ssRNA phage genomes. A simple way to identify chimeric genome assemblies is to count how many of the RNA genomes contain proteins with discordant phylogenies, that is, the co-occurrence of different subgroups of the core genes found in study [50]. Indeed, none of the 1398 complete genomes contained proteins with discordant phylogenies, and all contained exactly one copy of each core gene, except for one contig that contains a second RdRp gene after the first copy (RdRp B) that matches more closely to the other clade (RdRp A) (Additional File 1: Fig. S3). Additionally, the contig lengths of all tools are comparable, with PenguiN producing a somewhat higher fraction of genomes longer than 6 kbp than the other tools (Additional File 1: Fig. S4).

## Performance on 16S rRNA gene assembly

We then tested PenguiN's ability to recover the diverse 16S rRNA genes in metagenomic data. In general, 16S rRNA genes present difficulties for de Bruijn graph assemblers because they contain highly conserved regions interspersed with hypervariable sequences. By splitting reads into $k$-mers looses information needed to correctly connect conserved and the hypervariable regions when assembling contigs [44].

We detected 16S rRNA genes in the assemblies of the 82 metatranscriptomic samples described in the previous section using Barrnap, a tool that performs HMM searches using models derived from Rfam, SILVA, and RefSeq (https://github.com/tseemann/barrnap).

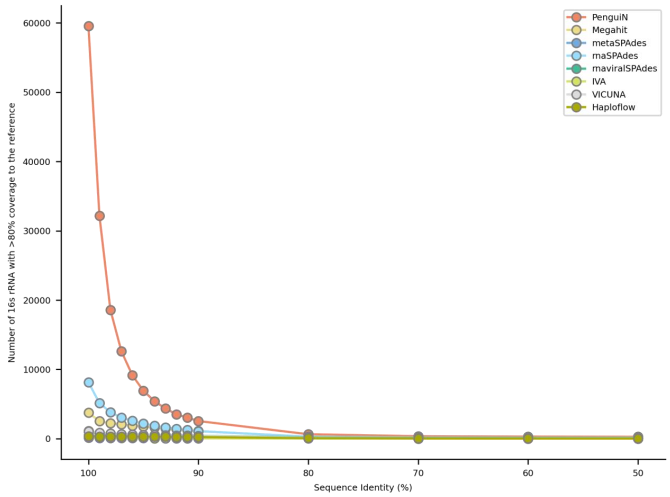


**Figure 8**: **Diversity of assembled 16S rRNA genes.** Number of 16S rRNA sequences in assembled contigs from different assemblers after clustering at different levels of sequence identity.

PenguiN was able to reconstruct 113 196 non-redundant 16S rRNAs gene fragments aligned to at least 50% of the Rfam database reference sequence (Fig. 7A). The second best tool in this category, rnaSPAdes, showed 18 933 matches ($\sim$ 6 times smaller number). For the matches with the coverage of at least 80% to the reference 16S rRNA genes (Fig. 7B), PenguiN again recovered 6 times more sequences, 32 169 against 5132 assembled with rnaSPAdes.

Cross-checking the Barrnap predictions (that only used Rfam database for 16S rRNA) with the SILVA database revealed the same pattern. The PenguiN-derived assembly has 20 923 and 6045 Barrnap hits with 99% identity to SILVA and at least 50% and at least 80% coverage, while rnaSPAdes has 2860 and 928 respectively (Fig. 7C,D).

The diversity of the reconstructed 16S rRNA genes (Fig. 8) was also significantly higher for PenguiN. For example, at 97% identity, PenguiN's assembly contained 12 616 16S rRNA genes while the next best tool, rnaSPAdes, contained only 3068. If we take 99% clustering identity as a threshold for defining species [54], then PenguiN reconstructed $\sim$ 6 times more species-level 16S rRNAs than rnaSPAdes (32 169 versus 5132).

# 3 Discussion

We presented PenguiN, the first overlap-based tool for strain-resolved viral genome and 16S rRNA assembly from metagenomic data. We compared it to nine state-of-the-art metagenomic and viral genome assemblers. On a simulated dataset with reads from 2550 HIV-1 genomes, PenguiN assembled a fraction of the HIV-1 genomes – matched at 99% sequence identity – that was many times higher and with much lower fragmentation than rnaSPAdes, the next best assembler. Despite its high sensitivity, PenguiN's precision (the fraction of assembled contigs that could be matched to one of the HIV-1 genomes) was similar to the state-of-the-art tools. PenguiN assembled around three times more complete ssRNA phage genomes from 82 samples from activated sludge and freshwater, with none of the 1398 complete genomes showing signs of chimerism (discordant protein sequence phylogenies). Penguin also assembled around seven times more full-length, bona-fide 16S rRNA sequences from the 82 metagenomic samples than the next best tool, rnaSPAdes.

When dealing with viral metagenomic data, the choice is between de Bruijn graph based metagenomic assemblers and virus-specific assemblers for low-complexity samples that mostly use overlap graphs. Our benchmarking results agree with results described in other studies [32, 55]: Due to the limitation of sequence context to the $k$-mer length, de Bruijn graph-based assemblers cannot phase highly similar genomes, while overlap based assemblers often cannot handle large and complex metagenomic samples.

PenguiN's use of the Linclust algorithm allows it to overcome the quadratic runtime complexity that plagues earlier overlap-based assemblers. In contrast, the other overlap assemblers we tested

needed either inordinate amounts of time or failed on the dataset of 82 metagenomics samples. Due to utilizing overlap alignments, PenguiN can make use of a much longer sequence context: the length of merged read pairs, and due to its Bayesian model to select the best sequences, it can exploit this longer context efficiently. The trend to increasing short read lengths – Illumina's current high-throuput sequencers NovaSeq 1000/2000 and 6000 can generate paired reads up to $2 \times 300$ and $2 \times 250$ base pairs, respectively – will further increase the length of PenguiN's sequence context and thus further improve its strain resolution compared to our benchmarks based on $2 \times 150$ paired reads.

Due to PenguiN's Bayesian selection and contig extension strategy, strain resolution is optimal when the coverage for a strain genome is at least 10, as in that case a read from the correct strain with good overlap to the contig is likely to be present in the dataset. When the coverage drops much below 10, the greedy extension strategy automatically falls back to reconstructing consensus sequences like other metagenomic assemblers do [44]. Our results show that, at low, medium and high read coverage, PenguiN produces similar amounts of assembly errors as the state of the art.

PenguiN has two main drawbacks. First, as shown in in Fig. 3b, its assemblies are slightly redundant, to a similar degree as the next best assembler in our benchmarks, rnaSPAdes. Second, and most importantly, PenguiN does not stop with its greedy extension when extensions are ambiguous. Therefore, it performs poorly when identical repeats or 100% conserved regions longer than the paired-read length are present in the metagenomes, since in this case PenguiN will randomly connect sequences upstream with sequences downstream. In preliminary experiments, this limitation led to suboptimal assemblies of some prokaryotic genomes. We are planning to address this limitation in the future by terminating the extension process when PenguiN detects a bifurcation, that is, two similarly good but incompatible extensions.

In conclusion, PenguiN is the first overlap-based assembler for viral genome and 16S rRNA assembly from large and complex metagenomic datasets. Due to analyzing all overlap alignments and a Bayesian strategy to select optimal extensions, it is able to assemble severalfold more strain-resolved genomes that the next best tool. The last decade has brought fascinating discoveries of a huge and often unexpected diversity of viruses in many different environments [6, 7, 8, 9, 10, 11, 12, 13, 14, 15, 16, 17, 18], and a large part of these successes were driven by progress in viral bioinformatics and computational tool development [56, 57]. We hope that PenguiN will make an important contribution to studying the roles of viruses on earth's microbiomes and to uncovering the molecular machinaries evolved by these most diverse and inventive of all biological entities.

# 4 Methods

## The protein-guided nucleotide assembly approach

PenguiN proceeds in two stages (Fig. **1**): In the protein-guided stage, it assembles six-frame translated protein sequences and co-assembles the corresponding nucleotide sequences. The resulting coding sequence-containing contigs are added to the original nucleotide reads and further assembled in the second stage. Each of the two stages consists of iterating the following two steps: (1) Find the overlaps among the working set of sequences that satisfy the specified criteria for extensions (maximum E-value, minimum sequence identity, and number of aligned residues), and (2) find the best upstream and downstream extensions to merge, and add the merged sequences into the working set. The two stages are now described in more detail (Additional File 1: Fig. S2).

In stage I, paired-end reads are merged, six-frame translation is performed, and potential ORFs are extracted. Then five iterations of overlap identification and extension are performed. First, protein overlaps are found in a time proportional to the number of sequences using the following Linclust algorithm [45]: A fixed number of $k$-mers (default: 60) are extracted from each sequence and stored in a reverse index table via a hash function value. This table is used to group sequences that share an identical $k$-mer substring ($k = 14$). The longest sequence per group, called center sequence, is selected, and groups with the same center sequence are merged together. Each center sequence is then aligned to each of the member sequences in its group. Because group member sequences are not aligned with each other, the algorithm achieves linear rather than quadratic time complexity. As in the protein-level assembler Plass [28], the alignments that satisfy the specified criteria of maximum E-value, minimum amino acid sequence identity, and minimum nucleotide sequence identity, are further considered as sequence extensions. Since we want to minimize the

risk of chimeric proteins that would lead to falsely connected nucleotide sequences, we chose strict default filter criteria of E-value $< 10^{-5}$, amino acid identity $> 97\%$, and a nucleotide identity of $> 99\%$. We select the best upstream extensions and the best downstream extensions according to a Bayesian posterior probability (see below). Each time two protein sequences are merged for extension, the corresponding nucleotide sequences are also extended in parallel. This stage ends after five iterations with pre-assembled contigs containing coding sequences.

In stage II, PenguiN links these pre-assembled contigs across intergenic regions. The coding sequence contigs are added to the original reads, and five iterations using the same greedy assembly procedure as in stage I are applied to the nucleotide sequences. To keep the specificity sufficiently high, a nucleotide $k$-mer size $k = 22$ is used in this stage. PenguiN again searches for overlaps in linear time and decides on the best sequence extensions based on the full alignments of the overlapping sequences. Again, the center sequences to be extended are the longest sequences in each group of sequences sharing a $k$-mer seed. In this way, we primarily extend contigs with other contigs and with non-coding reads, and, if there are no more pre-assembled contigs within the group, we also extend non-coding reads with non-coding reads. Since sequences and their reverse complements code for the same double-stranded DNA, we identify each $k$-mer with its reverse complement. We replace group member sequences with their reverse complement if their $k$-mer is the reverse complement of the matching $k$-mer in the center sequence. To maintain high sensitivity for identifying the overlaps, we scale the number of extracted seeds with the length of the sequences, by default we extract $0.1\times$ the number of residues in the sequence. In addition, we check for circular contigs after each iteration in stage II, because plasmids and many viral genomes are circular (see below). Since we cannot distinguish between circular genomes and perfect repeats, PenguiN will also stop extending contigs framed by two perfect repeats. Only the non-circular contigs are added to the working set to be further extended, while the circular ones are excluded from subsequent iterations and added directly to the output contigs.

For the final output, circular contigs collected over all iterations and linear contigs from the last iteration are combined. Since PenguiN is able to use reads more than once, the set of final contigs may be quite redundant. Therefore, in the last step, we perform a clustering of all final contigs using an extended version of Linclust [45] that takes circular contigs into account (option –wrapped-scoring), using a default maximum sequence identity of 99% and minimum coverage of 99% to obtain strain-resolved contigs. The longest sequence in each cluster is returned as result.

## Choosing extensions

PenguiN uses a Bayesian model to decide with which of several alternative choices of overlapping sequences to extend a center sequence. When overlap alignments differ markedly in length, this model improves upon the method used in Plass to simply pick the extension with the highest sequence identity. We can calculate the probability that the genome from one extending sequence has a higher sequence similarity with the genome of the center sequence than the genome from the other extending sequence.

Suppose we have a possible extension with $L$ overlapping, aligned nucleotides, of which $m$ are matches and $L - m$ are mismatches. The probability to observe $m$ matches among $L$ aligned residues is given by a binomal probability,

$$p(m|q, M) = \mathrm{Binom}(m|q, L)\,, \tag{1}$$

where $q$ is the unobserved, unknown average nucleotide identity (ANI) between the strains from which the two sequences originate. Using Bayes' theorem, we can calculate the posterior probability distribution of the ANI $q$ (see Additional File 1: Supp. Note 1),

$$p(q|m, L) = \mathrm{Beta}(q|m + a, L - m + b) \tag{2}$$

where we have assumed a prior distribution $p(q) = \mathrm{Beta}(q|a, b)$ with pseudocount parameters $a, b > 0$. Now suppose we have to decide which of two possible extending sequences to choose, one with $m_1$ matches out of $L_1$ aligned, overlapping residues and one with $m_2$ matches out of $L_2$ aligned residues. The probability that the ANI $q_1$ between the contig and the first extending sequence is lower than the ANI $q_2$ between the contig and the second extending sequence is

$$p(q_1 < q_2|m_1, L_1, m_2, L_2) = \int_0^1 \int_{q_1}^1 p(q_1|m_1, L_1)\, p(q_2|m_2, L_2)\; \mathrm{d}q_1\, \mathrm{d}q_2\,. \tag{3}$$

We show in the Supplemental Material how to analytically solve this integral and compute it efficiently. For the pseudocount parameters we choose $a = 1$, $b = 1$. Given this probability, we make the following choices when deciding if we want to preferably extend with an alignment $(m_1, L_1)$ rather than $(m_2, L_2)$: If $p(q_1 > q_2|m_1, L_1, m_2, L_2) > 0.55$ the first sequence is preferred for the extension, if $p(q_1 > q_2|m_1, L_1, m_2, L_2) < 0.45$ the second one is preferred. If the probability falls into the range 0.45 to 0.55 we consider it as "inconclusive", and prefer the extension that offers the longer extension instead. The center sequence is extended by the member sequence of its group that is preferred over all other possible extensions.

## Cycle detection

As circular and long terminal repeats are common among viruses and would lead to over-extensions in the greedy iterative assembly procedure, we introduced a step to detect contigs containing such structures. Therefore, we search for contigs with (near-)identical terminal repeats on both sides and exclude them from the next iterations. Instead, we mark them as circular and collect them over all iterations - marked by a flag in their header entry. To identify circular sequences while minimizing the runtime, we use a procedure that approximates the alignment of the sequence to itself using $k$-mer matches. We look for an overrepresentation of $k$-mer matches within diagonal bands and mark the contig as circular if a hit rate threshold of 0.24 is exceeded. This threshold was calculated using 5994 viruses from the RefSeq [58] database.

## Simulated datasets / Assembly benchmark

For benchmarking experiments, we generated synthetic read datasets. To make the distribution of the coding sequences as realistic as possible, we generated the reads from real viral genomes from the NCBI database [59]. For the first set (HRV in silico mixture), we downloaded three human rhinovirus strains (Accession No.: MF973193.1, MF973194.1, MN749156.1) with pairwise ANI values ranging from 92 to 95.5%. We mixed them in a proportion of 4:2:1 and simulated $2 \times 150$ bp overlapping paired-end reads (insert size range 220-280 bp) using randomreads.sh from the BBmap software suite (version 38.71) [60]. The simulated coverage was set to 50.

For the HIV datasets, we aimed to construct benchmark sets with a high degree of natural variation. We downloaded 2550 HIV-1 genomes from the NCBI database (accessed 07/2019, search string: ("Human immunodeficiency virus 1"[Organism] OR hiv1[All Fields]) AND complete genome[All Fields]). Comparing their ANI values with fastANI showed values mostly in the range from 85-95% (see Fig. **3**A). We then used randomreads.sh to generate three synthetic read datasets from this set using varying coverage values (1, 10, 100).

The HIV1 genome is approximately 9.7 kbp and is flanked at both ends by long terminal repeats (LTRs) that can interact, leading to circularized forms containing one or two copies of the viral LTR (1-LTR circles, 2-LTR circles) [47, 48]. All downloaded 2550 HIV-1 genomes were reported as "complete genome" in the NCBI database, but their LTRs were reported inconsistently (without, with one LTR or two LTRs, etc.). Because of that, it was not clear what result an assembler should ideally produce (genome with one LTR or two LTRs, etc.). Therefore, we consistently circularized all genomes by removing one of the repetitive regions, if two were present, and doubling the sequences, before simulating the reads. This results in reference genomes to which all linear representations of the complete genome can be mapped continuously, regardless of the starting position of the assembled contig.

We assembled all synthetic paired-end read datasets using PenguiN, Megahit, metaSPAdes, metaviralSPAdes, rnaSPAdes, rnaviralSPAdes, SAVAGE, IVA, VICUNA, and Haploflow.

## Evaluation on simulated datasets

For the evaluation of the assemblies, only contigs > 1 kb were considered. Evaluations of assemblies were performed with MetaQUAST [46], which provides commonly used statistics. We used MetaQUAST with the `--unique-maping` flag and default parameters otherwise as it is commonly used in metagenomic assembly benchmark studies [61, 32, 62]. In addition, we computed the per-base sensitivity and per-base precision values for the HIV datasets as we previously defined [28]. We searched with the set of reference genomes through the assembled contigs us-

ing MMseqs2 [49] with options -a -s 5.7 `--max-seqs 500000 --min-seq-id 0.89 --strand 2 --search-type 3 --max-seq-len 1000000` and subsequently filtered the resulting alignments with a minimum sequence identity threshold between 90% and 99%. Sensitivity was then calculated as the fraction of reference sequences that can be covered by contigs with a sequence identity of at least this threshold (total count of aligned nucleotides divided by the total length of the reference genomes). We considered two ways - either all alignments or only the longest alignment for each reference genome. Precision was calculated by searching with the contigs through the set of reference genomes, using MMseqs2 with options `-a -s 5.7 --max-seqs 5000 --min-ungapped-score 100 -a --min-seq-id 0.89 --strand 2 --search-type 3 --max-seq-len 10000000`. For each contig, only the longest alignment was considered. Precision was then defined as the fraction of contigs that are aligned to the reference genomes (total count of aligned nucleotides divided by total length of assembled contigs).

## Metatranscriptomic datasets

For the benchmark test on real sequencing data, we considered 82 metatranscriptomic samples from activated sludge and aquatic environments previously used in [50]. We downloaded the samples from the NCBI Sequence Read Archive (SRA) database and pre-processed them analogously to the Callanan et al. study. We removed Illumina adapters using Cutadapt (version 3.3) [63] and performed quality trimming using Trimmomatic (version 0.39) [64]. We discard all reads shorter than 100 bp. Assembly was then performed per sample using PenguiN, Megahit, metaSPAdes, metaviralSPAdes, rnaSPAdes, rnaviralSPAdes, SAVAGE, IVA, VICUNA, and Haploflow. The minimum contig length was set to 500 and the maximum runtime per sample was set to 10 days. We found that SAVAGE and IVA were unable to process the samples, so they were excluded from the results.

## Detecting ssRNA phage sequences in the assemblies

To detect and classify ssRNA phage contigs in the assemblies of the metatranscriptomic samples, we used the HMM based pipeline described in Callanan et al. [50] after the assembly. We predicted proteins with Prodigal (version 2.6.3) [65] and searched against the sequence profiles of the HMM 5-MC model generated by [50] using hmmscan from the HMMER package version 3.2.1 at http://hmmer.org/. Clustering was performed using MMseqs2. The sequence identity cutoff for clustering was first chosen as 100% in accordance to Callanan et al. However, for comparison between assemblers, we chose a cluster identity threshold of 99% to avoid overestimating sequences close to duplicates. All sequences longer than 750 bp were classified depending on the number of protein hits. We classified the contigs using the same terms as Callanan et al.: contigs encoding at least two protein hits ("partial genomes"), contigs encoding three protein hits ("near-complete genomes"), and contigs encoding three protein hits without proteins that are prematurely terminated by the edge of a contig ("complete genomes").

## Analysis of ssRNA phage sequences

Due to the lack of ground truth for real data, we could not calculate precision or sensitivity values, instead we assessed the assembly quality by analysing the complete ssRNA phage sequences in more detail. We calculated the fraction of PenguiN's assembled phage sequences which are covered by alignments to phage sequences in the other assemblies at a minimum identity cutoff of 99%. Aligning was performed using MMseq2 search [49] with options `--max-seqs 500000 -a --min-seq-id 0.99 --strand 2 --search-type 3 --min-aln-len 300 --max-seq-len 1000000`. To analyse the recovered diversity of the different assemblies we extracted from all complete phages the amino acid sequences that had a hit to the RdRp HMM model, and clustered them using MMseqs2 cluster [49] at sequence identity cutoffs of 50-100% (with step=10 until 90% and step=1 between 90 and 100%). To check the phylogenetic consistency we considered the subgroups of the three core genes that were observed to co-occur only in specific patterns [50]. We checked the order and co-occurrence of the core genes for deviations from these patterns using the list of predicted proteins provided by Prodigal and their respective HMM scores.

### Detecting 16S rRNA gene sequences in the assemblies

To detect 16S rRNA genes in the assemblies of the 82 metatranscriptomic samples, we used Barrnap v.0.9 (https://github.com/tseemann/barrnap). We classified predictions as being aligned to at least 80% or 50% of the reference 16S rRNA from the RFAM database v.11.0 [66]. To reduce redundancy, predicted 16S rRNA sequences were clustered using MMseqs2 with a sequence identity cutoff of 99%. To confirm the Barrnap predictions, we searched the detected 16S rRNA sequences (non-redundant) against the SILVA database v.138.1 [67]. The search was performed using MMseqs2 with a minimum sequence identity cutoff of 99%. To estimate the diversity of the 16S rRNA contigs, we clustered the sequences predicted by Barrnap using MMseqs2 with sequence identity cutoffs of 50-90% (with step = 10) and 91-99% (with step = 1). We then counted the number of cluster representatives having more than 80% of their sequence aligned to a reference 16S rRNA gene.

### Software

The respective software versions of the assembly tools used in the benchmark are: PenguiN (GitHub commit 7571d37), Megahit (v1.2.9), metaSPAdes/rnaSPAdes/metaviralSPAdes/rnaviralSPAdes (v3.15.2), SAVAGE (v0.4.2), IVA (v1.0.8), VICUNA (v1.3), Haploflow (v0.1).

Each assembler was run with default parameters, except for the minimum contig length and the CPU thread parameter setting, which was uniformly set to utilize all 16 available cores of the machine, if possible. The minimum contig length was set to 500 bp or 1000 bp depending on the dataset for all assemblers that provide such a filter option, or otherwise by filtering the final assembly file. As input, we used paired-end reads in two separate files or concatenated them if necessary.

### Acknowledgements

We thank Louis Kraft and Jinlong Ru for early testing of the software and giving feedback for parameter settings, and Bas Dutilh for feedback on the manuscript. JS acknowledges support by the ERC's Horizon 2020 Framework Programme ['Virus-X', project no. 685778] and the BMBF CompLifeSci project horizontal4meta. MS acknowledges support from the National Research Foundation of Korea (grants 2019R1A6A1A10073437, 2020M3A9G7103933, 2021R1C1C102065, and 2021M3A9I4021220), the Samsung DS Research Fund, and the Creative-Pioneering Researchers Program through Seoul National University.

### Author contributions

JS and MS conceived and supervised the research. AJ and MS developed the software. JS and EJ developed the Bayesian model for extension selection. AJ performed the virus data benchmarks. AJ and FAJ tested the software and analysed results. AK performed the 16S rRNA analysis. AJ and JS wrote the manuscript.

## Ethics approval and consent to participate

Not applicable.

### Competing interests

The authors declare that they have no competing interests.

### Data availability

All scripts and benchmark data including command-line parameters necessary to reproduce the benchmark and analysis results presented are available at https://github.com/AnnSeidel/penguin-analysis.

## Code availability

We integrated PenguiN into our Plass software. Source code and binaries are freely available under GPL-3.0 licence from https://github.com/soedinglab/plass. The latest released version is XXX. The source code used for benchmarking in this article can be accessed as git revision commit 7571d37. PenguiN is written in C++ and requires a 64-bit Linux/macOS system with at least SSE2 instructions

## Supplementary Information

## Additional File 1

Supplementary Figures S1-S4 and Supplementary Note 1.

# References


[1] S. Sunagawa, S. G. Acinas, P. Bork, C. Bowler, D. Eveillard, G. Gorsky, L. Guidi, D. Iudicone, E. Karsenti, et al., "Tara Oceans: towards global ocean ecosystems biology," Nature Rev Microbiol, vol. 18, no. 8, pp. 428–445, 2020.

[2] L. H. Morais, H. L. Schreiber IV, and S. K. Mazmanian, "The gut microbiota–brain axis in behaviour and brain disorders," Nature Rev Microbiol, vol. 19, no. 4, pp. 241–255, 2021.

[3] J. L. Round and S. K. Mazmanian, "The gut microbiota shapes intestinal immune responses during health and disease," Nature reviews immunology, vol. 9, no. 5, pp. 313–323, 2009.

[4] E. Amabebe, F. O. Robert, T. Agbalalah, and E. S. Orubu, "Microbial dysbiosis-induced obesity: role of gut microbiota in homoeostasis of energy metabolism," British J Nutrition, vol. 123, no. 10, pp. 1127–1137, 2020.

[5] S. Roux, J. Matthijnssens, and B. E. Dutilh, "Metagenomics in virology," Encyclopedia of Virology, p. 133, 2021.

[6] E. M. Adriaenssens, L. Van Zyl, P. De Maayer, E. Rubagotti, E. Rybicki, M. Tuffin, and D. A. Cowan, "Metagenomic analysis of the viral community in Namib Desert hypoliths," Environmental microbiology, vol. 17, no. 2, pp. 480–495, 2015.

[7] F. Schulz, L. Alteio, D. Goudeau, E. M. Ryan, F. B. Yu, R. R. Malmstrom, J. Blanchard, and T. Woyke, "Hidden diversity of soil giant viruses," Nature communications, vol. 9, no. 1, pp. 1–9, 2018.

[8] C. Santos-Medellin, L. A. Zinke, A. M. Ter Horst, D. L. Gelardi, S. J. Parikh, and J. B. Emerson, "Viromes outperform total metagenomes in revealing the spatiotemporal patterns of agricultural soil viral communities," ISME J, vol. 15, no. 7, pp. 1956–1970, 2021.

[9] S. Roux, J. R. Brum, B. E. Dutilh, S. Sunagawa, M. B. Duhaime, A. Loy, B. T. Poulos, N. Solonenko, E. Lara, J. Poulain, et al., "Ecogenomics and potential biogeochemical impacts of globally abundant ocean viruses," Nature, vol. 537, no. 7622, pp. 689–693, 2016.

[10] F. H. Coutinho, C. B. Silveira, G. B. Gregoracci, C. C. Thompson, R. A. Edwards, C. P. Brussaard, B. E. Dutilh, and F. L. Thompson, "Marine viruses discovered via metagenomics shed light on viral strategies throughout the oceans," Nature communications, vol. 8, no. 1, pp. 1–12, 2017.

[11] J. Hwang, S. Y. Park, M. Park, S. Lee, and T.-K. Lee, "Seasonal dynamics and metagenomic characterization of marine viruses in Goseong Bay, Korea," PloS one, vol. 12, no. 1, p. e0169841, 2017.

[12] A. C. Gregory, A. A. Zayed, N. Conceição-Neto, B. Temperton, B. Bolduc, A. Alberti, M. Ardyna, K. Arkhipova, M. Carmichael, C. Cruaud, et al., "Marine DNA viral macro-and microdiversity from pole to pole," Cell, vol. 177, no. 5, pp. 1109–1123, 2019.

[13] Y. I. Wolf, S. Silas, Y. Wang, S. Wu, M. Bocek, D. Kazlauskas, M. Krupovic, A. Fire, V. V. Dolja, and E. V. Koonin, "Doubling of the known set of RNA viruses by metagenomic analysis of an aquatic virome," Nature Microbiol, vol. 5, no. 10, pp. 1262–1270, 2020.

[14] A. A. Zayed, J. M. Wainaina, G. Dominguez-Huerta, E. Pelletier, J. Guo, M. Mohssen, F. Tian, A. A. Pratama, B. Bolduc, O. Zablocki, et al., "Cryptic and abundant marine viruses at the evolutionary origins of earth's rna virome," Science, vol. 376, no. 6589, pp. 156–162, 2022.

[15] A. N. Shkoporov, A. G. Clooney, T. D. Sutton, F. J. Ryan, K. M. Daly, J. A. Nolan, S. A. McDonnell, E. V. Khokhlova, L. A. Draper, A. Forde, et al., "The human gut virome is highly diverse, stable, and individual specific," Cell host & microbe, vol. 26, no. 4, pp. 527–541, 2019.

[16] A. C. Gregory, O. Zablocki, A. A. Zayed, A. Howell, B. Bolduc, and M. B. Sullivan, "The gut virome database reveals age-dependent patterns of virome diversity in the human gut," Cell host & microbe, vol. 28, no. 5, pp. 724–740, 2020.

[17] A. Gulyaeva, S. Garmaeva, R. A. Ruigrok, D. Wang, N. P. Riksen, M. G. Netea, C. Wijmenga, R. K. Weersma, J. Fu, A. V. Vila, et al., "Discovery, diversity, and functional associations of crAss-like phages in human gut metagenomes from four Dutch cohorts," Cell reports, vol. 38, no. 2, p. 110204, 2022.

[18] R. Li, Y. Wang, H. Hu, Y. Tan, and Y. Ma, "Metagenomic analysis reveals unexplored diversity of archaeal virome in the human gut," Nature Communications, vol. 13, no. 1, p. 7978, 2022.

[19] T. D. Sutton and C. Hill, "Gut bacteriophage: current understanding and challenges," Front Endocrinol, vol. 10, p. 490764, 2019.

[20] M. Breitbart, C. Bonnain, K. Malki, and N. A. Sawaya, "Phage puppet masters of the marine microbial realm," Nature microbiology, vol. 3, no. 7, pp. 754–766, 2018.

[21] E. V. Koonin, M. Krupovic, and V. V. Dolja, "The global virome: How much diversity and how many independent origins?," 2023.

[22] S. Nayfach, D. Páez-Espino, L. Call, S. J. Low, H. Sberro, N. N. Ivanova, A. D. Proal, M. A. Fischbach, A. S. Bhatt, P. Hugenholtz, et al., "Metagenomic compendium of 189,680 DNA viruses from the human gut microbiome," Nature Microbiology, vol. 6, no. 7, pp. 960–970, 2021.

[23] M. K. Mirzaei, J. Xue, R. Costa, J. Ru, S. Schulz, Z. E. Taranu, and L. Deng, "Challenges of studying the human virome–relevant emerging technologies," Trends in Microbiology, vol. 29, no. 2, pp. 171–181, 2021.

[24] M. Kleiner, L. V. Hooper, and B. A. Duerkop, "Evaluation of methods to purify virus-like particles for metagenomic sequencing of intestinal viromes," BMC genomics, vol. 16, pp. 1–15, 2015.

[25] R. Sanjuán and P. Domingo-Calap, "Mechanisms of viral mutation," Cellular and molecular life sciences, vol. 73, pp. 4433–4448, 2016.

[26] A. Kupczok, Z. M. Bailey, D. Refardt, and C. C. Wendling, "Co-transfer of functionally interdependent genes contributes to genome mosaicism in lambdoid phages," Microbial Genomics, vol. 8, no. 11, p. 000915, 2022.

[27] M. C. Schatz, A. L. Delcher, and S. L. Salzberg, "Assembly of large genomes using second-generation sequencing," Genome Res, vol. 20, no. 9, pp. 1165–1173, 2010.

[28] M. Steinegger, M. Mirdita, and J. Söding, "Protein-level assembly increases protein sequence recovery from metagenomic samples manyfold," Nature methods, vol. 16, no. 7, pp. 603–606, 2019.

[29] D. Li, C.-M. Liu, R. Luo, K. Sadakane, and T.-W. Lam, "MEGAHIT: an ultra-fast single-node solution for large and complex metagenomics assembly via succinct de Bruijn graph," Bioinformatics, vol. 31, no. 10, pp. 1674–1676, 2015.

[30] S. Nurk, D. Meleshko, A. Korobeynikov, and P. A. Pevzner, "metaSPAdes: a new versatile metagenomic assembler," Genome research, vol. 27, no. 5, pp. 824–834, 2017.

[31] E. Bushmanova, D. Antipov, A. Lapidus, and A. D. Prjibelski, "rnaSPAdes: a de novo transcriptome assembler and its application to RNA-Seq data," GigaScience, vol. 8, no. 9, p. giz100, 2019.

[32] T. D. Sutton, A. G. Clooney, F. J. Ryan, R. P. Ross, and C. Hill, "Choice of assembly software has a critical impact on virome characterisation," Microbiome, vol. 7, no. 1, pp. 1–15, 2019.

[33] D. Antipov, M. Raiko, A. Lapidus, and P. A. Pevzner, "Metaviral SPAdes: assembly of viruses from metagenomic data," Bioinformatics, vol. 36, no. 14, pp. 4126–4129, 2020.

[34] D. Meleshko, I. Hajirasouliha, and A. Korobeynikov, "coronaSPAdes: from biosynthetic gene clusters to RNA viral assemblies," Bioinformatics, vol. 38, no. 1, pp. 1–8, 2022.

[35] V. Mallawaarachchi, M. J. Roach, P. Decewicz, B. Papudeshi, S. K. Giles, S. R. Grigson, G. Bouras, R. D. Hesse, L. K. Inglis, A. L. Hutton, et al., "Phables: from fragmented assemblies to high-quality bacteriophage genomes," Bioinformatics, vol. 39, no. 10, p. btad586, 2023.

[36] A. Fritz, A. Bremges, Z.-L. Deng, T. R. Lesker, J. Götting, T. Ganzenmueller, A. Sczyrba, A. Dilthey, F. Klawonn, and A. C. McHardy, "Haploflow: Strain-resolved de novo assembly of viral genomes," Genome Biology, vol. 22, no. 1, pp. 1–19, 2021.

[37] A. H. Fitzpatrick, A. Rupnik, H. O'Shea, and P. Cotter, "High throughput sequencing for the detection and characterization of RNA viruses," Front Microbiol, vol. 12, p. 621719, 2021.

[38] J. A. Baaijens, A. Z. El Aabidine, E. Rivals, and A. Schönhuth, "De novo assembly of viral quasispecies using overlap graphs," Genome research, vol. 27, no. 5, pp. 835–848, 2017.

[39] R. Malhotra, M. M. S. Wu, A. Rodrigo, M. Poss, and R. Acharya, "Maximum likelihood de novo reconstruction of viral populations using paired end sequencing data," arXiv preprint arXiv:1502.04239, 2015.

[40] M. Hunt, A. Gall, S. H. Ong, J. Brener, B. Ferns, P. Goulder, E. Nastouli, J. A. Keane, P. Kellam, and T. D. Otto, "IVA: accurate de novo assembly of RNA virus genomes," Bioinformatics, vol. 31, no. 14, pp. 2374–2376, 2015.

[41] X. Yang, P. Charlebois, S. Gnerre, M. G. Coole, N. J. Lennon, J. Z. Levin, J. Qu, E. M. Ryan, M. C. Zody, and M. R. Henn, "De novo assembly of highly diverse viral populations," BMC genomics, vol. 13, no. 1, pp. 1–13, 2012.

[42] C. Yuan, J. Lei, J. Cole, and Y. Sun, "Reconstructing 16S rRNA genes in metagenomic data," Bioinformatics, vol. 31, no. 12, pp. i35–i43, 2015.

[43] C. S. Miller, B. J. Baker, B. C. Thomas, S. W. Singer, and J. F. Banfield, "EMIRGE: reconstruction of full-length ribosomal genes from microbial community short read sequencing data," Genome biology, vol. 12, no. 5, pp. 1–14, 2011.

[44] J. Vollmers, S. Wiegand, and A.-K. Kaster, "Comparing and Evaluating Metagenome Assembly Tools from a Microbiologist's Perspective - Not Only Size Matters!," PLoS ONE, vol. 12, no. 1, 2017.

[45] M. Steinegger and J. Söding, "Clustering huge protein sequence sets in linear time," Nature communications, vol. 9, no. 1, pp. 1–8, 2018.

[46] A. Mikheenko, V. Saveliev, and A. Gurevich, "MetaQUAST: evaluation of metagenome assemblies," Bioinformatics, vol. 32, no. 7, pp. 1088–1090, 2016.

[47] R. Craigie and F. D. Bushman, "Hiv dna integration," Cold Spring Harbor perspectives in medicine, vol. 2, no. 7, p. a006890, 2012.

[48] F. Maldarelli et al., "The role of HIV integration in viral persistence: no more whistling past the proviral graveyard," The Journal of clinical investigation, vol. 126, no. 2, pp. 438–447, 2016.

[49] M. Steinegger and J. Söding, "MMseqs2 enables sensitive protein sequence searching for the analysis of massive data sets," Nature biotechnology, vol. 35, no. 11, pp. 1026–1028, 2017.

[50] J. Callanan, S. R. Stockdale, A. Shkoporov, L. A. Draper, R. P. Ross, and C. Hill, "Expansion of known ssRNA phage genomes: from tens to over a thousand," Science advances, vol. 6, no. 6, p. eaay5981, 2020.

[51] Y. I. Wolf, D. Kazlauskas, J. Iranzo, A. Lucía-Sanz, J. H. Kuhn, M. Krupovic, V. V. Dolja, and E. V. Koonin, "Origins and evolution of the global RNA virome," MBio, vol. 9, no. 6, pp. e02329–18, 2018.

[52] K. Tars, "ssRNA Phages: Life Cycle, Structure and Applications," in Biocommunication of Phages, pp. 261–292, Springer, 2020.

[53] K. R. Chamakura, J. S. Tran, C. O'Leary, H. G. Lisciandro, S. F. Antillon, K. D. Garza, E. Tran, L. Min, and R. Young, "Rapid de novo evolution of lysis genes in single-stranded RNA phages," Nature communications, vol. 11, no. 1, pp. 1–11, 2020.

[54] R. C. Edgar, "Updating the 97% identity threshold for 16S ribosomal RNA OTUs ," Bioinformatics, vol. 34, pp. 2371–2375, 2018.

[55] Z.-L. Deng, A. Dhingra, A. Fritz, J. Götting, P. C. Münch, L. Steinbrück, T. F. Schulz, T. Ganzenmüller, and A. C. McHardy, "Evaluating assembly and variant calling software for strain-resolved analysis of large DNA viruses," Briefings in bioinformatics, vol. 22, no. 3, p. bbaa123, 2021.

[56] C. Lauber and S. Seitz, "Opportunities and challenges of data-driven virus discovery," Biomolecules, vol. 12, no. 8, p. 1073, 2022.

[57] E. V. Koonin and N. Yutin, "The crass-like phage group: how metagenomics reshaped the human virome," Trends in Microbiology, vol. 28, no. 5, pp. 349–359, 2020.

[58] N. A. O'Leary, M. W. Wright, J. R. Brister, S. Ciufo, D. Haddad, R. McVeigh, B. Rajput, B. Robbertse, B. Smith-White, D. Ako-Adjei, et al., "Reference sequence (RefSeq) database at NCBI: current status, taxonomic expansion, and functional annotation," Nucleic acids research, vol. 44, no. D1, pp. D733–D745, 2016.

[59] E. W. Sayers, M. Cavanaugh, K. Clark, J. Ostell, K. D. Pruitt, and I. Karsch-Mizrachi, "GenBank," Nucleic acids research, vol. 47, no. D1, pp. D94–D99, 2019.

[60] B. Bushnell, "BBMap: a fast, accurate, splice-aware aligner," tech. rep., Lawrence Berkeley National Lab.(LBNL), Berkeley, CA (United States), 2014.

[61] A. Sczyrba, P. Hofmann, P. Belmann, D. Koslicki, S. Janssen, J. Dröge, I. Gregor, S. Majda, J. Fiedler, E. Dahms, et al., "Critical assessment of metagenome interpretation—a benchmark of metagenomics software," Nature methods, vol. 14, no. 11, pp. 1063–1071, 2017.

[62] F. Meyer, A. Fritz, Z.-L. Deng, D. Koslicki, A. Gurevich, G. Robertson, M. Alser, D. Antipov, F. Beghini, D. Bertrand, et al., "Critical Assessment of Metagenome Interpretation-the second round of challenges," BioRxiv, 2021.

[63] M. Martin, "Cutadapt removes adapter sequences from high-throughput sequencing reads," EMBnet. journal, vol. 17, no. 1, pp. 10–12, 2011.

[64] A. M. Bolger, M. Lohse, and B. Usadel, "Trimmomatic: a flexible trimmer for Illumina sequence data," Bioinformatics, vol. 30, no. 15, pp. 2114–2120, 2014.

[65] D. Hyatt, G.-L. Chen, P. F. LoCascio, M. L. Land, F. W. Larimer, and L. J. Hauser, "Prodigal: prokaryotic gene recognition and translation initiation site identification," BMC bioinformatics, vol. 11, no. 1, pp. 1–11, 2010.

[66] S. W. Burge, J. Daub, R. Eberhardt, J. Tate, L. Barquist, E. P. Nawrocki, S. R. Eddy, P. P. Gardner, and A. Bateman, "Rfam 11.0: 10 years of RNA families," Nucleic Acids Research, vol. 41, no. D1, pp. D226–D232, 2013.

[67] C. Quast, E. Pruesse, P. Yilmaz, J. Gerken, T. Schweer, P. Yarza, J. Peplies, and F. O. Glöckner, "The SILVA ribosomal RNA gene database project: improved data processing and web-based tools," Nucleic Acids Research, vol. 41, no. D1, pp. D590–D596, 2013.